

# Improving ICP with Easy Implementation for Free Form Surface Matching\*

Yonghuai Liu<sup>†</sup>

Department of Computer Science  
The University of Wales, Aberystwyth  
Aberystwyth, SY23 3DB, UK  
Email: yyl@aber.ac.uk

## Abstract

Automatic range image registration and matching is an attractive but unresolved problem in both the machine vision and pattern recognition literature. Since automatic range image registration and matching is inherently a very difficult problem, the algorithms developed are becoming more and more complicated. In this paper, we propose a novel practical algorithm for automatic free-form surface matching. This method directly manipulates the possible point matches established by the traditional ICP criterion based on both the collinearity and closeness constraints without any feature extraction, image pre-processing, or motion estimation from outliers corrupted data. A comparative study based on a large number of real range images has shown the accuracy and robustness of the novel algorithm.

**Keywords** Collinearity constraint, closeness constraint, automatic matching, free form surface, ICP, motion consistency.

## 1 Introduction

In the last decade, laser range finders (range cameras) have been popular tools for scanning objects with free form surfaces. Since laser range finders can directly capture the depth information from the camera to the objects, the images captured are at least theoretically easier to analyse than projective images. Free form surfaces are represented as sets of structured 3D data points in the form of range images (Figure 1). Thus laser scanning systems provide fresh impetus for the fundamental research on 3D free form surface registration and matching in the machine vision and pattern recognition literature. Free form surface registration and matching has two goals: one is to determine correspondences between different data sets representing the same free form surface from different viewpoints, the other is to estimate the motion parameters bringing one data set into alignment with the other. In practice, these two goals are often interwoven, thus complicating free form surface matching. Registration and matching techniques find applications in many areas such as, for instance, object recognition, motion estimation, scene understanding, and computer aided geometric design (CAGD).

---

\*Pattern Recognition, Vol. 37, No. 3, pp. 211-226.

<sup>†</sup>Corresponding author. Tel.: +44 1970 621688; Fax: +44 1970 622455. Email: yyl@aber.ac.uk

## 1.1 Related work

Many methods have been proposed to tackle the registration problem, such as techniques based on the scatter matrix [1], iterative closest point (ICP) [2, 3, 4], extremal points [5], maximization of mutual information [6], interactive method [7], surface fitting [8], geometric histogram [9] and others. Among these methods, the ICP algorithm implements a natural idea: given motion parameters, for all points in the first image, the closest points in the second image to the transformed points must represent their correspondents. This idea is so practical and effective that it has attracted much attention from the machine vision and pattern recognition community. However, false matches occur in almost every iteration of the algorithm since unless the motion is tiny and no occlusion and appearance and disappearance of points occur, a single distance constraint cannot completely determine the position of correspondents in 3D space. As a result, a large number of techniques have been proposed to improve the traditional ICP algorithm. The main improvements to the traditional ICP algorithm are summarised in Table 1.

An overall analysis reveals that logically, there are two kinds of information that can be used to automatically match overlapping free form surfaces (Figure 2): one is the information extracted from a single image and the other is the information bridging points in different images. But these kinds of information cannot guarantee that the established correspondences between different free form surfaces are real. Thus, the key to successfully use these two kinds of information to match different free form surfaces is to eliminate false point matches. However under special situations, the correspondences between different images can be directly determined without the need to evaluate them. Thus, the existing free form surface matching algorithms can be classified into the following three basic categories, or a combination of them:

1. Structural consistency based methods [11, 12, 14, 18]. This class of methods have dominated image registration and matching techniques. The characteristics of this class of methods lie in that they assume that the objects are independent of viewpoints. As a result, the representation of object structure is independent of coordinate frames in which the object is described. In general they first extract some features from the structured data points and then examine the consistency between these features to establish or evaluate the possible point matches between different images. Structural consistency describes interpoint relationship in a single coordinate frame and it refers here not only to geometrical features, but also to optical features. The methods in this class have to deal with four primary problems: (1) the features to be extracted from images must be expressive in representing different views of objects; (2) the features to be extracted from images must be robust to noise, occlusion, and appearance and disappearance of points; (3) the similarity metric must be powerful in discriminating different features; and (4) since the features attached to a point in one image have to match those attached to each candidate in another, the established point matches could be completely wrong. Solving any of these problems is a challenging task;
2. Motion consistency based methods [27, 28, 29]. This class of methods are relatively new and need to be further explored. The characteristics of this class of methods lie in that they first use the traditional ICP criterion to establish a set of possible correspondences, then define a quality measurement for point matches based on rigid motion constraints and finally reject false matches based on their quality measurements. Rigid motion constraints describe the relationship between the point matches and the motion parameters

of interest. Since the algorithms can make full use of redundant data points for the estimation of the parameters of interest, they are in general accurate and robust. However, for accuracy and robustness, some parameters necessary for rejecting false matches must be properly defined; and finally

3. Mapping consistency based methods [1, 2, 15]. The characteristics of this class of methods lie in that they use a special mapping to determine point correspondences between the images to be registered. In order to make sure that the established correspondences are feasible, they often impose some constraints on image acquisition or require pre-processing of images. For example, the algorithm described in [1] assumes that the objects can be completely seen without occlusion and appearance and disappearance of points from two different viewpoints. The disadvantage of the existing methods in this class is that their assumptions are very restrictive.

The improvements to the traditional ICP algorithm can be reclassified in depth as follows:

- Increase the dimensionality of points from 3D [2, 3] to higher dimensions by incorporating other geometrical or optical features, such as normal vectors [10], laser reflectance strength value [16], colours [18], invariants [19] or curvature [20].
- Establish correspondences from matching points to matching curves [11, 12] to matching 2D images [13, 14].
- Establish correspondences from matching local structural features to examining motion consistency [27, 29] to combining both [31].
- Estimate motion parameters from using least squares method to using weighted least squares method [17], M-estimator [16] or simulated annealing [30].
- Estimate motion parameters from Euclidean space to frequency space [15].

From the above classification of the improvements, it can be seen that the algorithms developed are becoming more and more complicated. From machine learning theory [34], it is known that the more complex the algorithms are, the more likely the algorithms overfit the experimental data, and thus the less robust the algorithms are. Hence, while new methods and techniques need to be explored, we should not neglect the information in the existing algorithms that have not yet been fully investigated.

## 1.2 A novel solution

Given that the registration parameters rotation matrix  $\mathbf{R}$  and translation vector  $\mathbf{t}$  have been initialised or estimated, the traditional ICP criterion can be used to establish a set of possible correspondences  $(\mathbf{p}, \mathbf{p}')$  between the images to be registered. There are two basic different methodologies to evaluate whether or not a pair of points  $(\mathbf{p}, \mathbf{p}')$  represents a real correspondence: one methodology is to apply information associated with this pair of points without involving motion parameters. This corresponds essentially to the structural consistency based methods. The other is to apply information associated with this pair of points involving motion parameters. This corresponds essentially to the motion consistency based methods. The motion information involved in the latter methodology can be represented as rigid motion constraints bridging the points  $\mathbf{p}$  and  $\mathbf{p}'$  described in two different coordinate frames before and

after a rigid motion  $(\mathbf{R}, \mathbf{t})$ . Rigid motion constraints can be further classified into two categories: (1) rigid motion constraints involving the motion parameters that have to be estimated from the possible point matches  $(\mathbf{p}, \mathbf{p}')$  (this corresponds to the existing motion consistency based methods that have to estimate the motion parameters of interest such as the critical point [27] or the essential point [28, 29]); and (2) rigid motion constraints involving only the existing motion parameters  $(\mathbf{R}, \mathbf{t})$  without requiring motion estimation from the possible point matches  $(\mathbf{p}, \mathbf{p}')$ . The focus of this paper is to develop rigid motion constraints involving only the existing motion parameters for the evaluation of possible point matches established by the traditional ICP criterion for accurate and robust automatic free form surface matching.

The collinearity constraint is widely used to estimate the motion parameters in the object centred coordinate frame from a projective image [32, 33]. Unfortunately, to our knowledge, it has not yet been proposed that it be used for the evaluation of the established 3D-3D correspondences  $(\mathbf{p}, \mathbf{p}')$ . The collinearity constraint described in [33] means that the object point, the image point, and the optical centre are collinear. By analogy, given the motion parameters rotation matrix  $\mathbf{R}$  and translation vector  $\mathbf{t}$  for the registration and matching of free form surfaces, if  $(\mathbf{p}, \mathbf{p}')$  represent a real 3D-3D correspondence, then points  $\mathbf{R}\mathbf{p} + \mathbf{t}$ ,  $\mathbf{p}'$ , and the optical centre  $O$  should be as collinear as possible (due to noise,  $\mathbf{p}'$  is only approximately equal to  $\mathbf{R}\mathbf{p} + \mathbf{t}$ ). This means that the collinearity constraint is a necessary condition for  $(\mathbf{p}, \mathbf{p}')$  to represent a real correspondence. Hence the collinearity constraint can also be used to evaluate whether the possible point matches  $(\mathbf{p}, \mathbf{p}')$  between two range images to be registered represent real correspondences.

In this paper, we propose a novel motion consistency based approach to improve the traditional ICP algorithm for automatic free form surface matching without any feature extraction, image pre-processing, or motion estimation from the possible point matches  $(\mathbf{p}, \mathbf{p}')$ . This is in the spirit of the Occam's razor [34] in machine learning theory which claims that simpler algorithms are preferred. The novel approach makes full use of both the collinearity and closeness constraints to evaluate the possible correspondences  $(\mathbf{p}, \mathbf{p}')$  established by the traditional ICP criterion. The collinearity constraint minimises the distance between the transformed point  $\mathbf{R}\mathbf{p} + \mathbf{t}$  and the ray passing through  $\mathbf{p}'$ . The closeness constraint minimises the distance between points  $\mathbf{R}\mathbf{p} + \mathbf{t}$  and  $\mathbf{p}'$ . The implementation of the collinearity constraint is in agreement with the assumption that the scanning error occurs mainly along the ray shooting from the range camera [24]. In order to improve the robustness of the proposed algorithm, when we have detected that the algorithm is about to terminate, we add a tiny perturbation to the estimated motion parameters so that the algorithm is forced to search for an optimal solution in the neighbouring region of the estimated motion parameters. The novel algorithm not only can deal with occlusion, appearance and disappearance of points, but also has the advantage of easy implementation since it is based on the rigid motion constraints involving just the existing motion parameters rotation matrix  $\mathbf{R}$  and translation vector  $\mathbf{t}$ .

For a comparative study of performance, we also implemented another two algorithms: one is the Pulli pair-wise registration algorithm [25] based on traditional ICP and orientation consistency examination and the other is the motion consistency based GICP algorithm [28]. While the Pulli algorithm was initialised by the GICP algorithm, the initialisation of the novel algorithm was the same as for the GICP algorithm. Different algorithms have different criteria to define point correspondences. In order to overcome the bias toward different numbers of finally established correspondences, we propose to normalise the performance measurement for different free form surface matching algorithms. The normalisation is implemented through computing the parameters of interest uniformly based on the reciprocal correspondences [35],

rather than on the correspondences defined or refined by different algorithms. Since reciprocal correspondences are one-to-one mapping established correspondences [29] that tend to represent the overlapping area between the free form surfaces to be matched, are completely determined by the motion parameters calibrated by different free form surface matching algorithms and their determination involves no thresholds set by the user, they provide a more objective and accurate measurement of the performance of different free form surface matching and registration algorithms. A large number of experiments based on real images have indeed demonstrated the advantages of the novel algorithm. Thus we argue that future research may focus on tiny motion registration and matching with occlusion and appearance and disappearance of points, rather than on initialisation of the traditional ICP algorithm.

The rest of this paper is organised as follows. Section 2 proposes the novel algorithm, Section 3 presents experimental results, and Section 4 analyses the reasons why the novel algorithm does work. Finally, some conclusions are drawn in Section 5.

## 2 The novel algorithm

Assume that the given two images to be matched can be described as point sets  $\mathbf{P} = \{\mathbf{p}_1, \mathbf{p}_2, \dots, \mathbf{p}_{n_1}\}$  and  $\mathbf{P}' = \{\mathbf{p}'_1, \mathbf{p}'_2, \dots, \mathbf{p}'_{n_2}\}$ . Due to occlusion, appearance and disappearance of points,  $n_1$  is not necessarily equal to  $n_2$ . The sizes of  $n_1$  and  $n_2$  depend on the representation accuracy required to approximate the free form surfaces to be matched. The points in the two images with the same subscript do not mean that they represent 3D correspondences. Given the registration parameters rotation matrix  $\mathbf{R}$  and translation vector  $\mathbf{t}$ , for any point  $\mathbf{p}_i$  in the first image  $\mathbf{P}$ , the traditional ICP algorithm uses the following criterion to determine its possible correspondent  $\mathbf{p}'_i$  in the second image  $\mathbf{P}'$ :

$$\mathbf{p}'_i = \underset{\mathbf{p}' \in \mathbf{P}'}{\operatorname{argmin}} \|\mathbf{p}' - \mathbf{R}\mathbf{p}_i - \mathbf{t}\| \quad (1)$$

which minimises the Euclidean distance between the transformed point  $\mathbf{R}\mathbf{p}_i + \mathbf{t}$  and  $\mathbf{p}'$  in the second image  $\mathbf{P}'$ . The search space is determined by the size of the second image  $\mathbf{P}'$ . Due to inaccurate initial motion parameters, occlusion, appearance and disappearance of points and noise distribution in image data, some point matches  $(\mathbf{p}_i, \mathbf{p}'_i)$  established by this criterion must be false matches. Thus a large number of techniques (as described in the last section) have been proposed to evaluate whether the point pair  $(\mathbf{p}_i, \mathbf{p}'_i)$  represents a real correspondence. To this end, all these methods have to either extract features from images or estimate the motion parameters of interest from the false matches corrupted correspondence data  $(\mathbf{p}_i, \mathbf{p}'_i)$ . Unfortunately, both feature extraction from images and motion estimation from the outliers corrupted data  $(\mathbf{p}_i, \mathbf{p}'_i)$  are challenging tasks themselves in the machine vision and pattern recognition community. Thus, in this paper, we propose *directly* manipulating the possible correspondences  $(\mathbf{p}_i, \mathbf{p}'_i)$  without feature extraction and motion estimation, while still achieving accurate and robust automatic free form surface registration and matching.

Given that the registration parameters rotation matrix  $\mathbf{R}$  and translation vector  $\mathbf{t}$  have been initialised or estimated, based on the ICP criterion (Equation 1), a set of possible point correspondences  $(\mathbf{p}_i, \mathbf{p}'_i)(i = 1, 2, \dots, n_1)$  between images  $\mathbf{P}$  and  $\mathbf{P}'$  to be registered can be established. For each possible correspondence  $(\mathbf{p}_i, \mathbf{p}'_i)$ , if they represent a real correspondence, then points  $\mathbf{R}\mathbf{p}_i + \mathbf{t}$ ,  $\mathbf{p}'_i$  and the optical centre  $O$  are as collinear as possible and the distance between points  $\mathbf{R}\mathbf{p}_i + \mathbf{t}$  and  $\mathbf{p}'_i$  is as small as possible. For the sake of reference, the former is called the *collinearity* constraint and the latter is called the *closeness* constraint. Since, at the

beginning of matching, the motion parameters rotation matrix  $\mathbf{R}$  and translation vector  $\mathbf{t}$  are not accurate, the established correspondences  $(\mathbf{p}_i, \mathbf{p}'_i)$  are just pseudo correspondences since in the strict sense, none of them may represent a real correspondence. However, we can compute these two constraints as a quality measurement of possible point matches  $(\mathbf{p}_i, \mathbf{p}'_i)$  from which relatively good matches can be selected and used for motion re-estimation. To this end, the transformed first image points and the second image points are all synthesised into the same coordinate system. The consequence of this synthesis is to normalise the imaging process in which, while the cameras keep static, the objects are in motion. For each possible point match  $(\mathbf{p}_i, \mathbf{p}'_i)$ , the collinearity constraint is computed as the distance  $d_i$  (collinearity error) between transformed point  $\mathbf{R}\mathbf{p}_i + \mathbf{t}$  and the ray passing through  $\mathbf{p}'_i$  and the closeness constraint as the distance  $e_i$  (registration error) between points  $\mathbf{p}'_i$  and  $\mathbf{R}\mathbf{p}_i + \mathbf{t}$  (Figure 3):

$$d_i = (|\|\mathbf{p}'_i - \mathbf{R}\mathbf{p}_i - \mathbf{t}\|^2 - \frac{(\mathbf{p}'_i{}^T(\mathbf{R}\mathbf{p}_i + \mathbf{t}))^2}{\mathbf{p}'_i{}^T\mathbf{p}'_i}|)^{0.5}, \quad e_i = \|\mathbf{p}'_i - (\mathbf{R}\mathbf{p}_i + \mathbf{t})\|$$

where  $\|\mathbf{x}\|$  denotes the Euclidean norm of vector  $\mathbf{x}$ ,  $|x|$  denotes the absolute value of scalar  $x$ , and superscript  $T$  denotes transpose.  $d_i$  and  $e_i$  are measurements of the quality of possible point matches  $(\mathbf{p}_i, \mathbf{p}'_i)$ . The smaller  $d_i$  and  $e_i$ , the better the possible point match  $(\mathbf{p}_i, \mathbf{p}'_i)$ . If  $(\mathbf{p}_i, \mathbf{p}'_i)$  represents a real correspondence, then both  $d_i$  and  $e_i$  are small positive real numbers due to noise in the imaging process.

Then we compute the means  $\mu_d$  and  $\mu_e$  and standard deviations  $\sigma_d$  and  $\sigma_e$  of  $d_i$  and  $e_i$  respectively over the possible point matches in which no points lie on boundaries. Finally we use the following rule to reject false matches: If  $|d_i - \mu_d| \leq \kappa\sigma_d$ ,  $|e_i - \mu_e| \leq \kappa\sigma_e$ , and both  $\mathbf{p}_i$  and  $\mathbf{p}'_i$  are non-boundary points, then  $(\mathbf{p}_i, \mathbf{p}'_i)$  is regarded as a feasible correspondence. Otherwise, it is regarded as a false one. As a result of this procedure, a set of refined correspondences is obtained from which the quaternion method [2] can be used to re-estimate the registration parameters rotation matrix  $\mathbf{R}$  and translation vector  $\mathbf{t}$ .

Parameter  $\kappa$  here plays an important role in rejecting false matches [27, 29]. If it is set too large, then false matches remain. If it is set too small, then good matches are rejected. All these cases will bias the algorithm for motion estimation. Our experience has shown that when  $\kappa$  is defined in the interval [1.0, 2.0], good free form surface matching results can be expected. In the experiments described in the next section, we let  $\kappa = 1.4$ .

The above procedure can be iterated until convergence. In this paper, either when the variation of the average registration errors between two successive iterations is smaller than the desired registration error  $\epsilon$  and the variation of either the rotation or translation vector at two successive iterations is smaller than  $\rho$ , or when the iteration number is larger than the maximum  $M$ , the algorithm terminates. Parameters  $\epsilon$  and  $\rho$  here again cannot be set too large or too small [27, 29]. If they are set too large, then the algorithm can converge prematurely at an early stage, leading to inaccurate free form surface matching results. If they are set too small, then the algorithm requires more intensive computation or even diverges or fluctuates in some extreme cases. Our experience has shown that when they are defined within the intervals  $\epsilon \in [0.00001, 0.001]$  and  $\rho \in [0.001, 0.005]$ , good free form surface registration and matching results can be achieved. In the experiments as described below, the following values were used:  $\epsilon = 0.0001$ ,  $\rho = 0.001$ , and  $M = 200$ .

Sometimes, however, the proposed algorithm does get stuck at a local minimum, leading to inaccurate image registration and matching results. In order to overcome this problem, when we have detected that the algorithm is about to terminate and the maximum iteration

number  $M$  has not yet been reached, we add a small perturbation to the estimated motion parameters quaternion  $\hat{\mathbf{q}} = (q_0, q_1, q_2, q_3)^T$ , representing rotation matrix  $\mathbf{R}$ , and translation vector  $\hat{\mathbf{t}} = (t_1, t_2, t_3)^T$ :

$$q_i \leftarrow q_i * (1 + \delta q_i) (i = 0, 1, 2, 3), \quad t_j \leftarrow t_j * (1 + \delta t_j) (j = 1, 2, 3)$$

where  $\delta q_i$  and  $\delta t_j$  are small real numbers. Since the calibrated quaternion  $\hat{\mathbf{q}}$  should be of unit length, renormalization is thus required:  $\hat{\mathbf{q}} \leftarrow \hat{\mathbf{q}} / \|\hat{\mathbf{q}}\|$ .  $\delta q_i$  and  $\delta t_j$  again cannot be set too large or too small. If they are set too large, then the algorithm has to repeat the free form surface matching process from a quite different solution without making full use of the existing relatively good one and this leads the algorithm to be less efficient. If they are set too small, then no significantly different solution is examined and thus, no better solution will be found. In the experiments as described in the next section,  $\delta q_i$  and  $\delta t_j$  were randomly generated with uniform distribution within the interval  $[-0.0025, 0.0025]$ . Then we apply the perturbed registration parameters to the first image points and re-compute the variation of the parameters of interest at two successive iterations and repeat the steps as described above.

The idea of this perturbation is similar to a genetic algorithm [22] and simulated annealing [30] where a number of candidates for registration parameters generated from the neighbouring region of the estimated solution are examined so that the global optimal solution can be found. Such a perturbation has two roles:

1. It helps the algorithm to traverse the local minimum, leading to more accurate image registration and matching results. This is demonstrated in Figure 4, from which it can be clearly seen that the algorithm converged to a local minimum. The perturbation forced the algorithm to repeat the image matching process from a nearby solution. Eventually, the algorithm has yielded a more accurate motion estimation result with a smaller image matching error.
2. It helps the algorithm to verify the existing image matching, leading to more reliable matching results. This is demonstrated in Figures 6 and 8. In these two cases, the image registration and matching is already accurate. So the algorithm performed a few more iterations to verify the existing image registration and matching results.

The improved ICP algorithm is called the Collinear ICP (CICP) algorithm. From the above description, it can be seen that the CICP algorithm is easy to implement, since it is just based on the information provided by the ICP criterion (Equation 1) without requiring any feature extraction, image pre-processing, or motion estimation from the possible point matches  $(\mathbf{p}_i, \mathbf{p}'_i)$ . When the algorithm is about to terminate, a little perturbation is added to the estimated motion parameters. However, the CICP algorithm does provide very good results for automatic free form surface registration and matching as demonstrated in the next section.

### 3 Experimental Results

For a better understanding of the performance of the CICP algorithm, we also implemented the GICP algorithm [28] and the Pulli algorithm [25] on a Pentium III, 500 MHz computer. The initialisation parameters were used as described in [28] where  $\mathbf{q}^{(0)} = (\sqrt{99}/10, 0.1, 0, 0)^T$  and  $\mathbf{t}^{(0)} = \bar{\mathbf{p}}' - \bar{\mathbf{p}}$  and  $\bar{\mathbf{p}}'$  and  $\bar{\mathbf{p}}$  are centroids of the second and first images, respectively. We carried out a large number of experiments based on real images and all the experiments exhibit similar

behaviour. Due to space limit, we here just present three representative experiments. The real range images depicted in Figure 1 and Table 2 were downloaded from the range image database hosted by the Signal Analysis and Machine Perception Laboratory at Ohio State University. The images were acquired using a Minolta 700 range scanner with a resolution of  $200 \times 200$  pixels. From the name encoding of image files, the rotation angle about an unknown rotation axis can be derived. Even though an accurate rotation angle in practice is difficult to measure, it does provide a rough reference for the measurement of the performance of different algorithms. Both the CICIP and GICIP algorithms were directly applied to the image data without any image pre-processing or feature extraction and also without any knowledge about occlusion, appearance and disappearance of points, or exact motion information. Thus the experiments based on such images represent typical imaging conditions and can provide an objective evaluation of different algorithms. In this paper, a boundary point is defined as the one with at least one of its eight nearest neighbours in the raster image file invalid. The parameters of interest in this paper are the average collinearity error  $\mu_d$ , the calibrated rotation angle  $\hat{\theta}$  and the average registration error  $\mu_e$  based on refined correspondences. The evolution of the parameters of interest are presented in Figures 4, 6 and 8. In the figures, the solid lines correspond to the CICIP algorithm, the dash lines correspond to the GICIP algorithm, the lines with pluses correspond to the Pulli algorithm. For better visualisation effect, we randomly selected with uniform distribution 200 points from the first tubby, cow and bunny images and their evolutions of matching are presented in Figures 5, 7 and 9, respectively. In the figures, the pluses represent the transformed first image points, circles represent the second image points. The statistics of image matching results are presented in Tables 3 and 4.

From Figures 4, 6 and 8, it can be seen that at the beginning of registration, the calibrated rotation angles  $\hat{\theta}$  are small and both the average collinearity error  $\mu_d$  and the average registration error  $\mu_e$  are large. As the registration progresses, even though the calibrated rotation angles  $\hat{\theta}$  are not monotonically increasing and neither the average collinearity error  $\mu_d$  nor the average registration error  $\mu_e$  is monotonically decreasing about the iteration numbers, the overall trend is that the calibrated rotation angles  $\hat{\theta}$  approach the expected ones and both the average collinearity error  $\mu_d$  and the average registration error  $\mu_e$  become smaller and smaller. These figures clearly show the desired evolutionary behaviour of free form surface matching algorithms.

In Figures 4 and 6, the perturbation positions can be easily recognised. While the CICIP algorithm converged to a local minimum for the registration of tubby images, due to perturbation of the estimated motion parameters, the CICIP algorithm successfully traversed that local minimum, leading to more accurate free form surface matching and motion estimation results. In contrast, the perturbation forced the CICIP algorithm to carry out a few more iterations to verify the existing cow image registration results. However, in Figure 8, the perturbation position (at iteration 47) is not easily recognisable. This can be explained as follows. The parameters of interest are functions of refined correspondences. The determination of refined correspondences depends not only on the perturbed motion parameters, but the geometry of the free form surface as well. In the case of the registration of bunny images, the perturbation does not lead to significantly different refined correspondences, yielding much different calibration of the parameters of interest. Even so, the perturbation is large enough to force the CICIP algorithm to carry out a few more iterations, searching for an optimal solution in the neighbouring region of the estimated motion parameters.

From Figures 4, 6, and 8 and Table 3, it can be seen that for bunny images, all algorithms have obtained small average registration errors and the calibrated rotation angles are close

to  $20^\circ$  as expected. This shows that high quality images are easy to match. From Figure 1, it can be seen that two tubby images are very similar despite the fact that they were taken from two different viewpoints. As a result, the GICP algorithm has difficulty in registering the images. This phenomenon is clearly illustrated by Figure 4 and Table 3 where the GICP algorithm converges at a very early stage with an average registration error of 0.41mm. After the coarse matching has been refined by the Pulli algorithm, the results have been improved. However, the result is not perfect since the rotation angle still has an error of 6.10%. So two similar tubby images lead both the GICP and Pulli algorithms to get stuck at local minima leading to inaccurate image matching results. For cow images, even though the calibrated rotation angles are all close to the expected  $30^\circ$ , all algorithms have obtained relatively large average registration errors. This shows that the resolution of cow images is not as high as that of either the bunny or tubby images (Table 2). From this, we can conclude that poor quality images are difficult to match and often lead different algorithms to show a large variation among the matching results. Therefore, it will be useful to investigate methods to measure the quality of images in future so that the image matching quality can be predicted before the image matching process actually takes place [27, 29].

From Figures 5, 7 and 9, it can be seen that at the beginning of registration, the two sets of image points show considerable difference in 3D space. But after registration, the two sets of points are perfectly matched and appearing and disappearing points can be clearly seen. This visual validation clearly conveys the quality of free form surface matching and shows that the CICP algorithm is accurate and robust for the automatic matching of free form surfaces as demonstrated in this paper.

From Figures 4, 6 and 8 and Table 3, it can be seen that the Pulli algorithm is the most accurate in the sense of average registration error based on refined correspondences for the registration of range images used in this paper. This is because it removed worst 10% point matches and established a limited number of correspondences. Our experience has shown that the Pulli algorithm has two shortcomings: one is that it requires a good initialisation of motion parameters; the other is that when a good initialisation of motion parameters is provided, it cannot guarantee to improve the coarse registration results significantly. What is worse is that it sometimes fails to register the images. However, from Table 4, it can be clearly seen that even though the CICP algorithm has been initialised by a solution which is far from correct, it is the most accurate and robust algorithm in the sense of average registration error based on *reciprocal* correspondences [35] for automatic free form surface matching. This shows that a combination of the collinearity constraint with the closeness constraint is powerful in evaluating the possible point correspondences established by the traditional ICP criterion (Equation 1). Since we do not know the exact motion parameters, we cannot exactly measure the performance of the proposed algorithm but we believe that the CICP algorithm is capable of providing a good initialisation for other even more accurate algorithms and future research may focus on the matching of free form surfaces undergoing tiny motions with occlusion and appearance and disappearance of points, rather than on how to initialise the traditional ICP algorithm. Table 4 shows that different algorithms establish similar number of reciprocal correspondences between different images. This is because they were used to match the same free form surface.

## 4 Analysis of the Novel Algorithm

From the description of the novel CICIP algorithm, it is known that it has the advantage of easy implementation, while retaining the computational complexity  $O(n_1n_2)$  of the traditional ICP algorithm (where  $n_1$  and  $n_2$  denote the numbers of valid points in the first and second images, respectively). But the experiments based on real images have shown that it is very accurate and robust for automatic free form surface matching, overcoming the shortcomings of both the GICP and Pulli algorithms, since the former can easily get stuck at a local minimum and the latter requires a good initialisation of motion parameters. We analyse the CICIP algorithm as follows.

In order to evaluate the possible correspondences  $(\mathbf{p}_i, \mathbf{p}'_i)$  between the free form surfaces to be matched, the CICIP algorithm iteratively minimizes the collinearity error  $d_i$  between point  $\mathbf{R}\mathbf{p}_i + \mathbf{t}$  and the ray passing through  $\mathbf{p}'_i$  and the registration error  $e_i$  between  $\mathbf{p}'_i$  and  $\mathbf{R}\mathbf{p}_i + \mathbf{t}$  for each possible point match  $(\mathbf{p}_i, \mathbf{p}'_i)$ . In essence,  $d_i$  and  $e_i$  define the quality of point matches  $(\mathbf{p}_i, \mathbf{p}'_i)$ . The smaller  $d_i$  and  $e_i$ , the better the point match  $(\mathbf{p}_i, \mathbf{p}'_i)$ . In the ideal case, both  $d_i$  and  $e_i$  are zero. At the beginning of matching, since the motion parameters rotation matrix  $\mathbf{R}$  and translation vector  $\mathbf{t}$  are not accurate, the average collinearity error  $\mu_d$  and the average registration error  $\mu_e$  are large as illustrated by Figures 4, 6 and 8. But as the registration progresses, the calibrated motion parameters become more and more accurate and thus, as expected, leading both the average collinearity error  $\mu_d$  and the registration error  $\mu_e$  to become smaller and smaller. Assume that eventually, more than three point matches  $(\mathbf{p}_i, \mathbf{p}'_i)$  have registration errors  $e_i$  of zero and these points are not collinear:  $\mathbf{p}'_i = \mathbf{R}\mathbf{p}_i + \mathbf{t}$ , then the registration parameters rotation matrix  $\mathbf{R}$  and translation vector  $\mathbf{t}$  are uniquely determined and point matches  $(\mathbf{p}_i, \mathbf{p}'_i)$  do represent real correspondences. From Figure 3 and the definitions of the collinearity error  $d_i$  and the registration error  $e_i$ , it is known that  $0 \leq d_i \leq e_i$ . Since  $e_i = 0$ , thus  $d_i = 0$ . This shows that points  $\mathbf{R}\mathbf{p}_i + \mathbf{t}$ ,  $\mathbf{p}'_i$ , and the optical centre  $O$  are collinear. Hence, in this case, the collinearity constraint provides additional assurance that the found point match  $(\mathbf{p}_i, \mathbf{p}'_i)$  is real.

In practice, the imaging process often introduces, to data points, noise caused by sampling, discontinuity of edges, various optical reflection characteristics of surfaces, etc. Even though the free form surface matching is perfect, the corresponding points are not always exactly superposed and thus, in this case, small registration errors occur. However, the closeness constraint only constrains the possible correspondents lying on the spheres centred at the transformed points (Figure 3), the collinearity constraint only constrains the possible correspondents lying on the cones with the apexes at the optical centre  $O$  and the centre axes defined as the rays passing through the transformed points. Neither the point far away from the transformed point nor the point through which a ray passes and the ray is distant from the transformed point is a possible correspondent. Only both constraints can then accurately constrain the possible correspondents close to the transformed points and near the rays passing through the transformed points and thus, leading to more accurate and robust free form surface matching results. The implementation of the collinearity constraint is justified by the assumption that the scanning error occurs mainly along the ray shooting from the camera [24].

In the case where the algorithm has got stuck at a local minimum, then it still has an opportunity to traverse that local minimum by using the perturbation of the motion parameters. So, the perturbation provides again additional assurance that the algorithm will converge to a correct solution. The experimental results based on a large number of real images have

shown that such a strategy is effective for automatic free form surface matching.

## 5 Conclusions

The main contribution of this paper can be summarised as two aspects:

1. We have proposed a novel practical algorithm for automatic free-form surface matching. The novel algorithm directly manipulates the possible point matches established by the traditional ICP criterion (Equation 1) based on both the collinearity and closeness constraints. In contrast with the existing structural consistency based methods, the novel algorithm does not require any feature extraction, or image pre-processing. In contrast with the existing motion consistency based methods, the novel algorithm does not require motion estimation from the possible correspondences before they are evaluated. And finally, in contrast with the existing mapping consistency based methods, the novel algorithm can deal with occlusion and appearance and disappearance of points. As a result, the novel algorithm inherits the compactness of the traditional ICP algorithm and has the advantage of easy implementation;
2. We have proposed normalising the performance measurement for different free form surface matching algorithms uniformly based on reciprocal correspondences [35]. Since reciprocal correspondences are one-to-one mapping established correspondences [29] that tend to represent the overlapping area between the free form surfaces to be matched, are completely determined by the motion parameters calibrated by different free form surface matching algorithms and their determination involves no thresholds setup by the user, they provide a more objective and accurate performance measurement for different free form surface matching and registration algorithms.

A large number of experiments based on real images have shown that even though it was initialised by a solution which is far from correct, the novel CICIP algorithm is very accurate and robust for automatic free form surface matching.

Further research will: (1) investigate the methods to improve the computational efficiency of the novel algorithm based on techniques such as K-D tree [4, 18]; (2) investigate the methods for the measurement of image quality so that image matching quality can be predicted before the matching process actually occurs; (3) fine tune the parameter  $\kappa$  so that more accurate and robust matching results can be obtained. To this end, it will be useful to consider the quality of images; and finally (4) investigate the methods to match free form surfaces undergoing tiny motions with occlusion and appearance and disappearance of points. Research is underway and the results will be reported in future.

## Acknowledgements

We would like to express our sincere thanks to the anonymous referee for his/her valuable comments and to Dr Lynda Thomas from the University of Wales at Aberystwyth for her proofreading of the paper.

## References

- [1] Z. Lin et al, Finding 3D point correspondences in motion estimation. *Proc. 8th ICPR*, 1986, pp. 303-305.
- [2] P.J. Besl, N.D. McKay, A method for registration of 3D surfaces, *IEEE Trans. PAMI*, 14(2)(1992) 239-256.
- [3] Y. Chen and G. Medioni, Object modelling by registration of multiple range images, *IVC*, 10(1992) 145-155.
- [4] Z. Zhang, Iterative point matching for registration of free-form curves. *Technical report*, no. 1658, INRIA, France, 1992.
- [5] J.P. Thirion, New feature points based on geometric invariants for 3D image registration. *Technical Report*, no. 1901, INRIA, France, 1993.
- [6] P. Viola and W.M. Wells III, Alignment by maximization of mutual information. *Proc. ICCV*, 1995, pp. 16-23.
- [7] P.J. Neugebauer, Reconstruction of real world objects via simultaneous registration and robust combination of multiple range images, *Int. Journal of Shape Modelling*, 3(1997) 71-90.
- [8] J.P. Tarel, H. Civi, and D.B. Cooper, Pose estimation of free form 3D objects without point matching using algebraic surface models. *Proc. IEEE Workshop on Model Based 3D Image Analysis*, 1998, pp. 13-21.
- [9] A.P. Ashbrook, R.B. Fisher, C. Robertson, and N. Werghi, Finding surface correspondences for object recognition and registration using pair-wise geometric histogram. *Proc. 5th ECCV*, 1998, vol. II, pp. 185-201.
- [10] J. Feldmar, N. Ayache, and F. Betting, 3D-2D projective registration of free-form curves and surfaces, *CVIU*, 65(1997) 403-424.
- [11] Y. Sun and M.A. Abidi, Surface matching by 3D point's fingerprint. *Proc. ICCV*, 2001, pp. 263-269.
- [12] J.V. Wyngaerd, L.V. Gool, B. Koch, and M. Proesmans, Invariant-based registration of surface patches. *Proc. ICCV*, 1999, pp. 301-306.
- [13] S.M. Yamany and A.A. Farag, Surface signatures: an orientation independent free-form surface representation scheme for the purpose of objects registration and matching, *IEEE Trans. PAMI*, 24(2002) 1105-1120.
- [14] D. Huber, O. Carmichael, and M. Hebert, 3D map reconstruction from range data. *Proc. ICRA*, 2000, pp. 891-897.
- [15] L. Lucchese, G. Doretto, and G.M. Cortelazzo, A frequency domain technique for range image registration, *IEEE Trans. PAMI*, 24(11)(2002) 1468-1484.
- [16] K. Nishino and K. Ikeuchi, Robust simultaneous registration of multiple range images. *Proc. 5th ACCV*, 2002, pp. 454-461.
- [17] G. Turk and M. Levoy, Zippered polygon meshes from range images. *Proc. SIGGRAPH*, 1994, pp. 311-318.

- [18] A.E. Johnson and S.B. Kang, Registration and integration of textured 3-D data, *IVC*, 17(1999) 135-147.
- [19] G.C. Sharp, S.W. Lee, and W.K. Wehe, Invariant features and the registration of rigid bodies, *IEEE Trans. PAMI*, 24(2002) 90-112.
- [20] R. Yang and P.K. Allen, Registering, integrating, and building CAD models from range data. *Proc. ICRA*, 1998, pp. 3115-3120.
- [21] S.M. Yamany, M.N. Ahmed, E.E. Hemayed, and A.A. Farag, Novel surface registration using the grid closest point transform. *Proc. ICIP*, 1998, pp. 809-813.
- [22] K. Brunnstrom and A.J. Stoddart, Genetic algorithms for free-form surface matching. *Proc. ICPR*, 1996, pp. 689-693.
- [23] S. Rusinkiewicz and M. Levoy, Efficient variants of the ICP algorithm. *Proc. Int. Conf. 3DIM*, 2001, pp. 145-152.
- [24] R. Sagawa, T. Osihi, A. Nakazawa, R. Kurazume, K. Ikeuhi, Iterative refinement of range images with anisotropic error distribution. *Proc. IEEE/RSJ IROS*, 2002, pp. 79-85.
- [25] K. Pulli, Multiview registration for large data sets. *Proc. Int. Conf. 3DIM*, 1999, pp. 160-168.
- [26] C. Dorai, G. Wang, A.K. Jain, and C. Mercer, From Images to models: automatic model construction from multiple views. *Proc. ICPR*, 1996, pp. 770-774.
- [27] Y. Liu and M.A. Rodrigues, Geometrical analysis of two sets of 3D correspondence data patterns for the registration of free-form shapes, *J. Int. and Rob. Systems*, 33(2002) 409-436.
- [28] Y. Liu, M.A. Rodrigues, and Y. Wang, Developing rigid motion constraints for the registration of free-form shapes. *Proc. IEEE/RSJ IROS*, 2000, pp. 2280-2285.
- [29] M.A. Rodrigues and Y. Liu, On the representation of rigid body transformations for accurate registration of free form shapes, *Robotics and Autonomous Systems*, 39(1)(2002) 37-52.
- [30] J. Luck, C. Little, and W. Hoff, Registration of range data using a hybrid simulated annealing and iterative closest point algorithm. *Proc. ICRA*, 2000, pp. 3739-3744.
- [31] Y. Liu, M.A. Rodrigues, Accurate registration of structured data using two overlapping range images. *Proc. ICRA*, 2002, vol. 3, pp. 2519-2524.
- [32] Y. Liu and H. Holstein, A pseudo linearization method for accurate pose estimation from a single image. *Proc. ICIP*, 2002, vol. 2, pp. 557-560.
- [33] B. Rosenhahn, Y. Wen, G. Sommer, Performance of constraint based pose estimation algorithms. *Proc. DAGM Symposium*, 2000, pp. 277-284.
- [34] T.M. Mitchell, *Machining learning*. McGraw-Hill Companies, Inc. 1997.
- [35] T. Pajdla, L. Van Gool, Registration of 3-D Curves Using Semi-differential Invariants. *Proc. ICCV*, 1995, pp. 390-395.

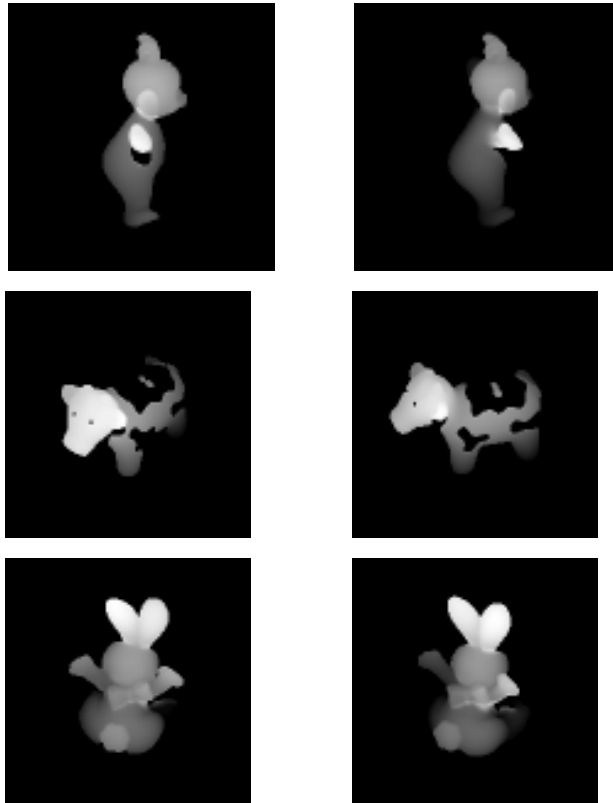


Figure 1: The real range images used. Top: tubby; Middle: cow; Bottom: bunny.

## Vitae

Yonghuai Liu received his PhD degree from Department of Computer Science at The University of Hull, United Kingdom in 2000. Then he was employed as a research fellow at Computing Research Centre of Sheffield Hallam University, United Kingdom. Since September 2001, he has been working as a lecturer at Department of Computer Science of The University of Wales, Aberystwyth, Wales, United Kingdom. He was a guest editor for the special issue on the registration and fusion of range images of the Computer Vision and Image Understanding journal. He has published more than 60 papers in image registration, motion estimation and artificial intelligence. He is a member of the IEEE.

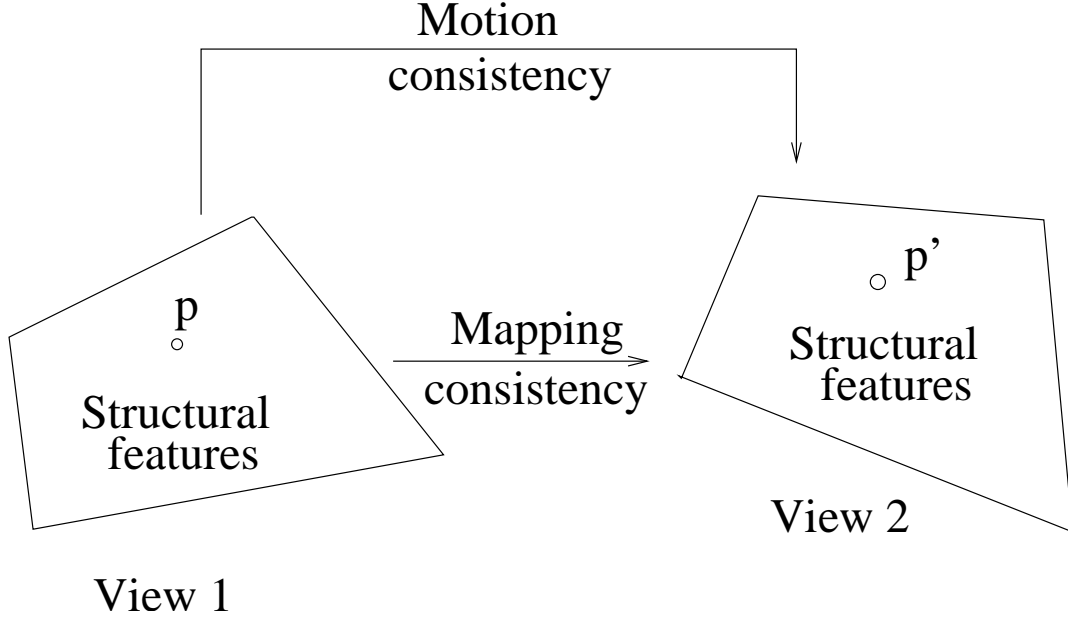


Figure 2: The classification of improvements of the traditional ICP algorithm.

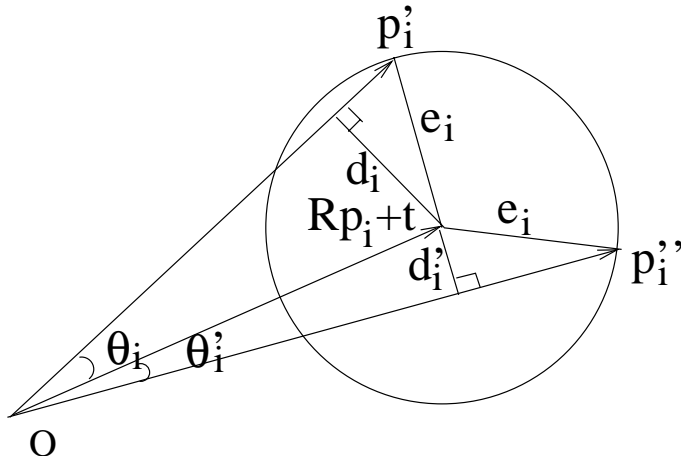


Figure 3: The collinearity and closeness constraints. With the same registration error  $e_i$ , point  $\mathbf{p}_i''$  is a preferred correspondent of point  $\mathbf{p}_i$  since  $d_i' < d_i$  and  $\theta_i' < \theta_i$  and thus, the transformed point  $\mathbf{R}\mathbf{p}_i + \mathbf{t}$  is closer to the ray passing through  $\mathbf{p}_i''$  than to the ray passing through  $\mathbf{p}_i'$ , where  $d_i'$  and  $d_i$  are the distances from point  $\mathbf{R}\mathbf{p}_i + \mathbf{t}$  to the rays passing through  $\mathbf{p}_i''$  and  $\mathbf{p}_i'$ ,  $\theta_i'$  and  $\theta_i$  are the including angles between point vector  $\mathbf{R}\mathbf{p}_i + \mathbf{t}$  and point vectors  $\mathbf{p}_i''$  and  $\mathbf{p}_i'$  respectively.

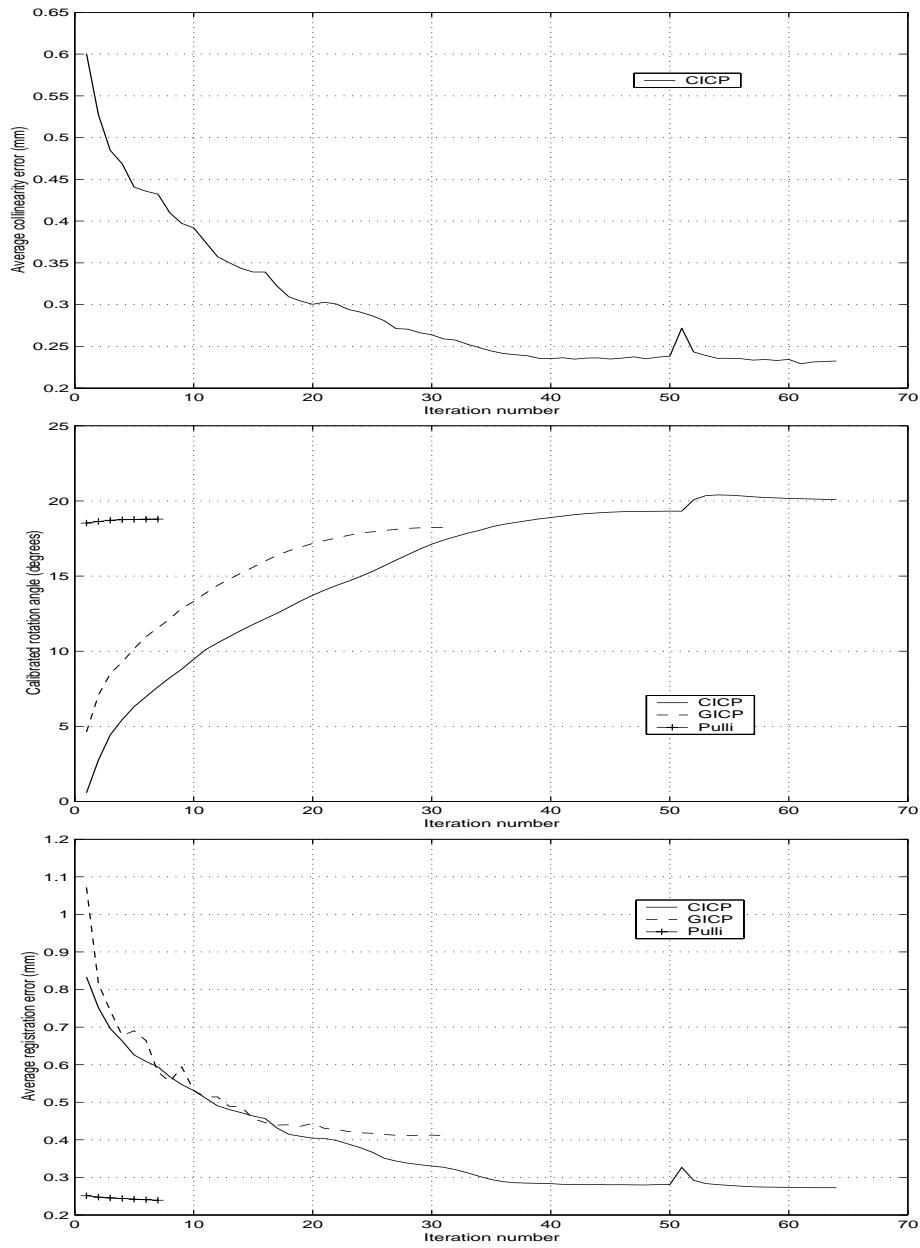


Figure 4: Tubby images: the evolution of the parameters of interest at different iterations for different algorithms. Top: average collinearity error; Middle: calibrated rotation angle; Bottom: average registration error.

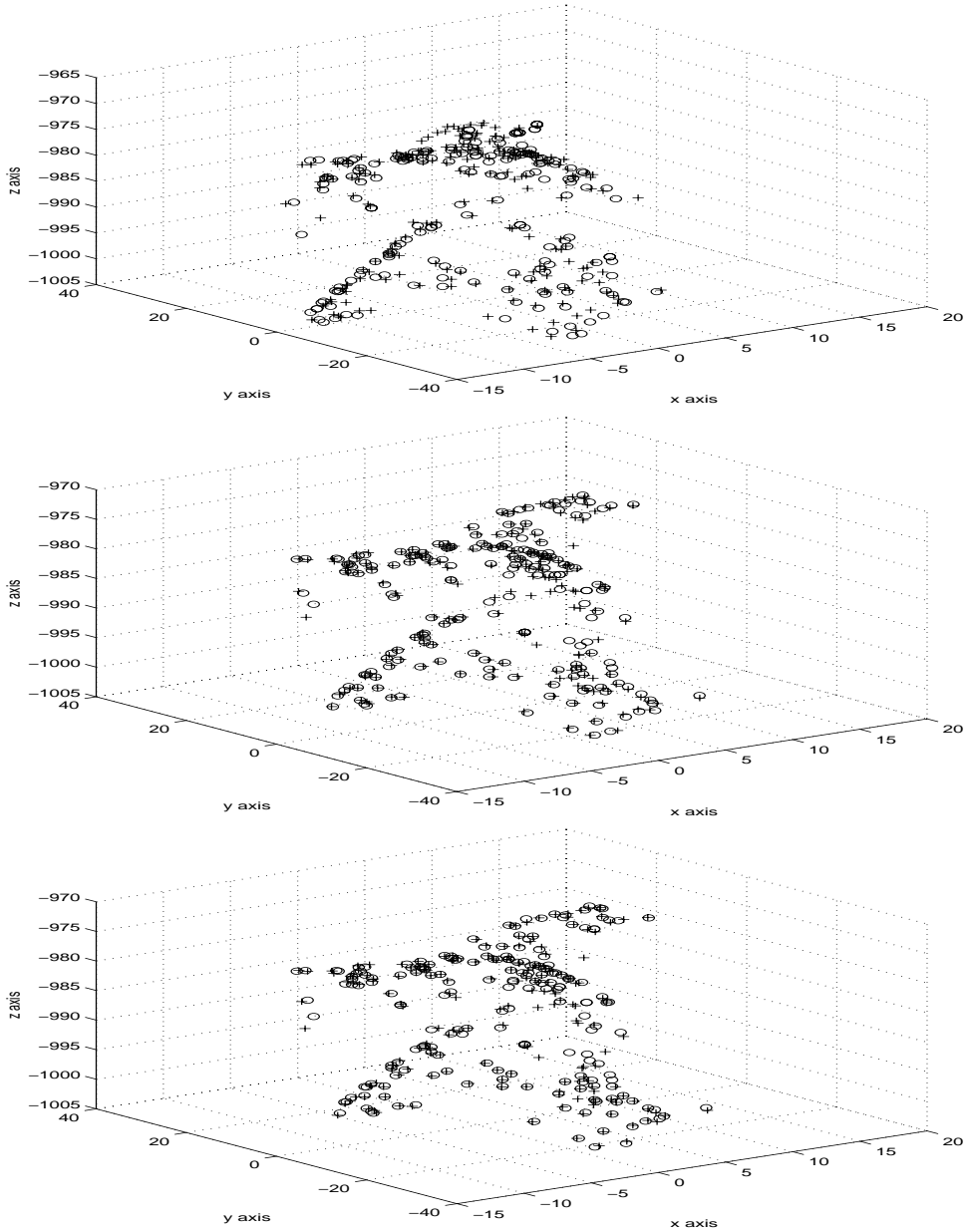


Figure 5: The evolution of the registration of 200 points randomly selected with uniform distribution from the first tubby image for the CICP algorithm. Top: registration at iteration 1; Middle: registration at iteration 32; Bottom: final registration 150 points out of 200 in the first tubby image find their correspondents in the second tubby image. The pluses represent the transformed first image points, circles represent the second image points.

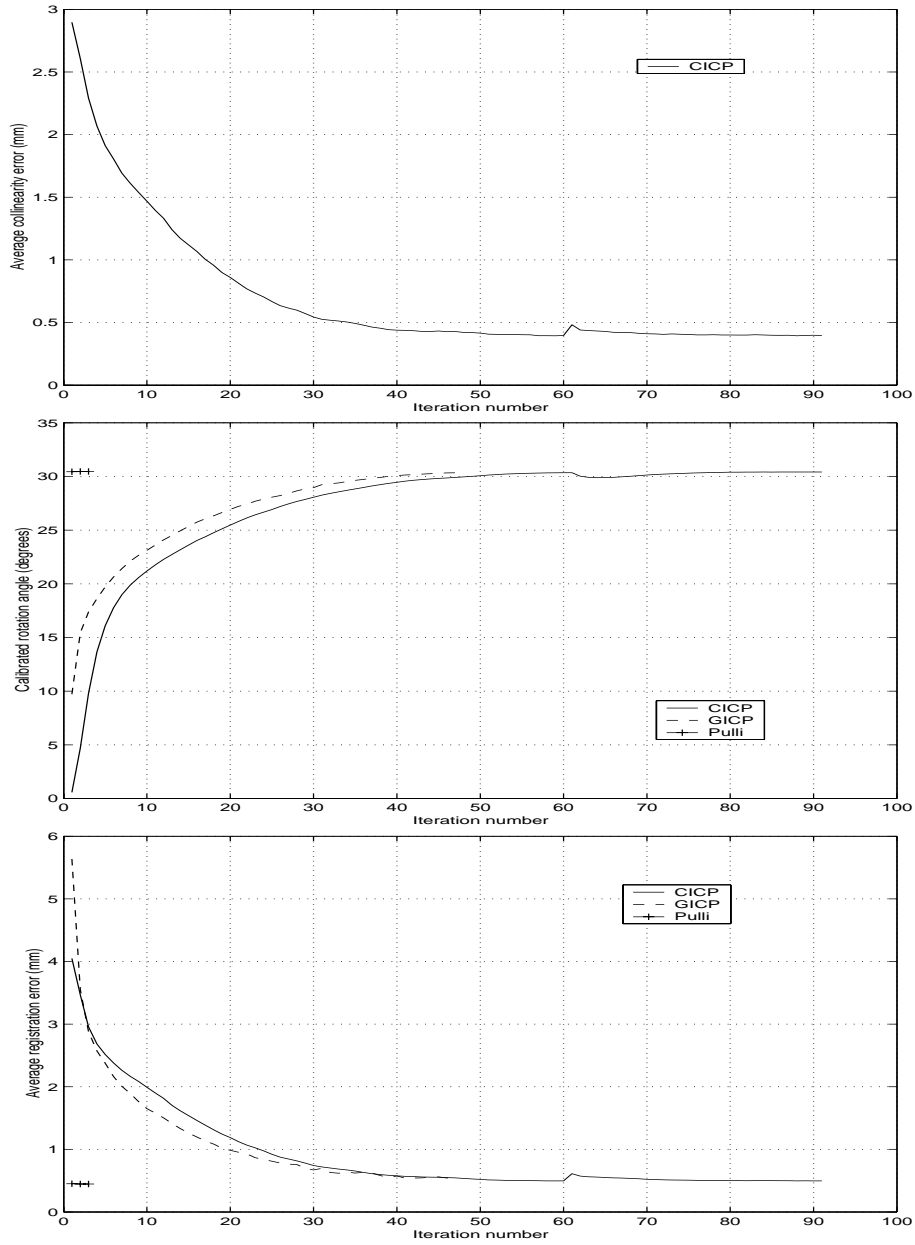


Figure 6: Cow images: the evolution of the parameters of interest at different iterations for different algorithms. Top: average collinearity error; Middle: calibrated rotation angle; Bottom: average registration error.

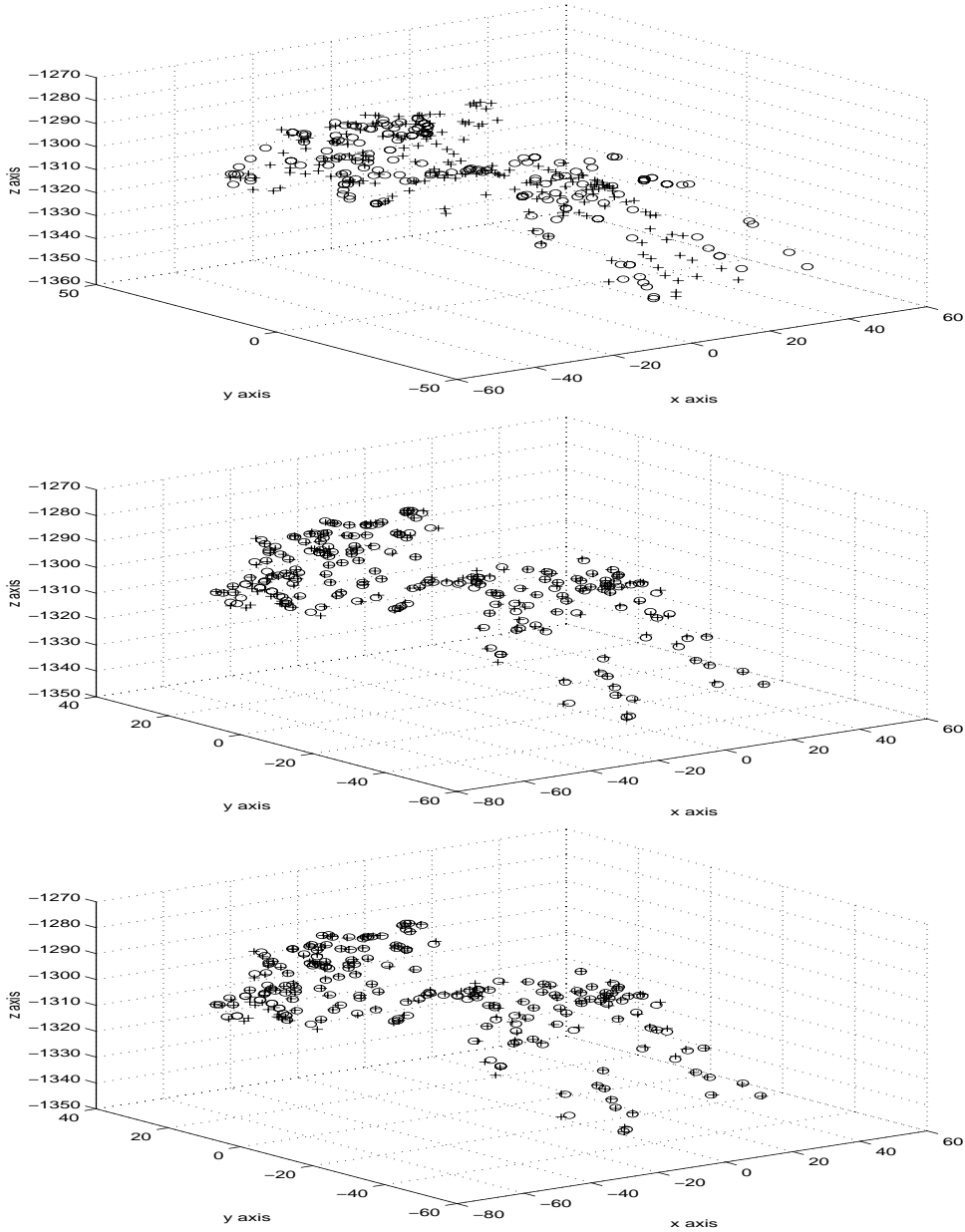


Figure 7: The evolution of the registration of 200 points randomly selected with uniform distribution from the first cow image for the CIP algorithm. Top: registration at iteration 1; Middle: registration at iteration 45; Bottom: final registration 138 points out of 200 in the first cow image find their correspondents in the second cow image. The pluses represent the transformed first image points, circles represent the second image points.

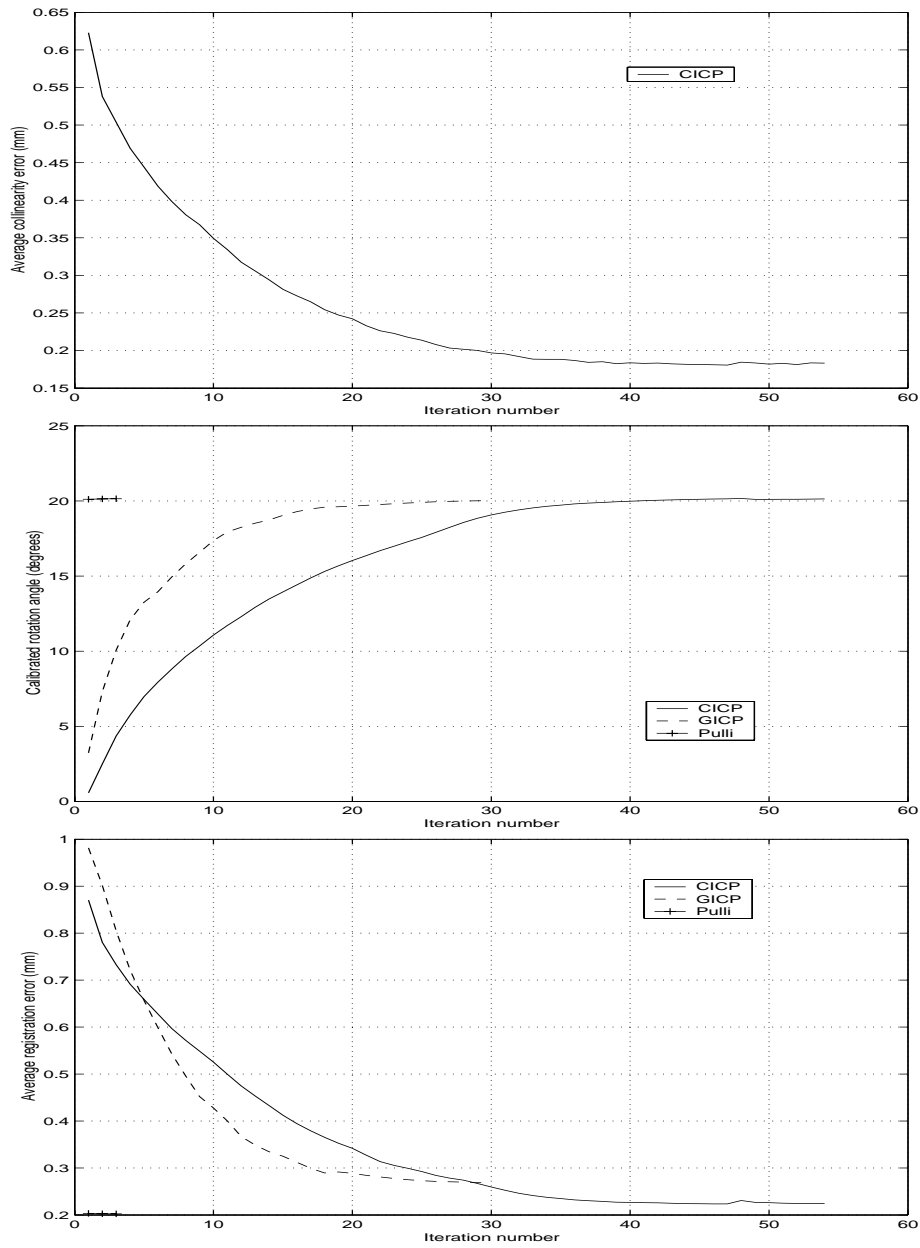


Figure 8: Bunny images: the evolution of the parameters of interest at different iterations for different algorithms. Top: average collinearity error; Middle: calibrated rotation angle; Bottom: average registration error.

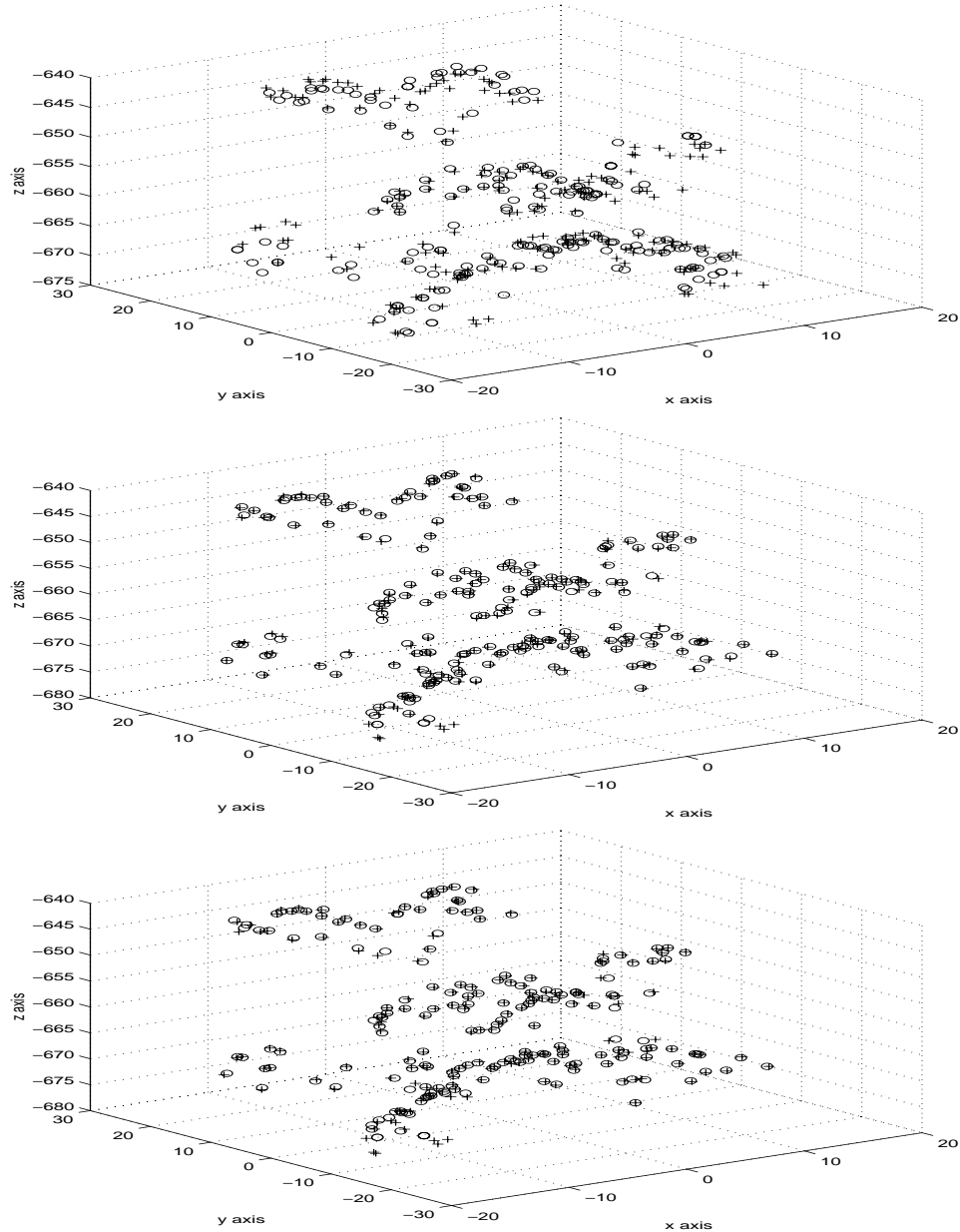


Figure 9: The evolution of the registration of 200 points randomly selected with uniform distribution from the first bunny image for the CICP algorithm. Top: registration at iteration 1; Middle: registration at iteration 27; Bottom: final registration 147 points out of 200 in the first bunny image find their correspondents in the second bunny image. The pluses represent the transformed first image points, circles represent the second image points.

Table 1: Techniques used to improve the traditional ICP algorithm.

components	techniques
initialisation	distance matching [10]
	fingerprint matching [11]
	bitangent curve matching [12]
	surface signature matching [13]
	spin image matching [14]
	Fourier transform [15]
distance measurement	laser reflectance strength [16]
	point to triangular mesh [17]
	colour [18]
	normal vector [10]
	invariants [19]
	curvature weighted distance [20]
closest point search	constrained nearest point [17]
	K-D tree [18]
	grid closest point [21]
	genetic algorithm [22]
false matches rejection	discarding boundary points [17, 23]
	threshold [18, 24]
	normal vectors [25]
	point-to-point distance consistency [26]
	orientation consistency [4]
	correspondence vectors [27]
	reflected correspondence vectors [28, 29]
motion estimation	M-estimator [16]
	simulated annealing estimation [30]
	weighted least squares [17]
	Extended Kalman Filter [10]

Table 2: The number of valid points  $N$ , the average  $\mu_l$  and standard deviation  $\sigma_l$  of interpoint distances in millimetres in different images.

Image	Viewpoint	$N$	$\mu_l(mm)$	$\sigma_l(mm)$
tubby	1	4354	0.80	0.39
	2	4361	0.89	0.66
cow	1	4262	1.59	0.79
	2	4864	1.57	0.62
bunny	1	6870	0.69	0.35
	2	6874	0.67	0.28

Table 3: The mean  $\mu_e$  and standard deviation  $\sigma_e$  of registration errors in millimetres, expected rotation angle  $\theta$  and calibrated rotation angle  $\hat{\theta}$  in degrees, the number  $N$  of finally established correspondences and the registration time in seconds for different algorithms applied to different range images.

Image	Algo.	$\mu_e(mm)$	$\sigma_e(mm)$	$\theta(^{\circ})$	$\hat{\theta}(^{\circ})$	$N$	time(s)
tubby	CICP	0.27	0.14	20	20.09	3161	127
	GICP	0.41	0.48		18.23	4001	67
	Pulli	0.24	0.09		18.78	1411	19
cow	CICP	0.50	0.16	30	30.41	2915	179
	GICP	0.56	0.25		30.34	3795	100
	Pulli	0.45	0.16		30.46	106	10
bunny	CICP	0.22	0.09	20	20.14	5291	251
	GICP	0.27	0.16		20.02	6338	151
	Pulli	0.20	0.08		20.15	3194	27

Table 4: The mean  $\mu_e$  and standard deviation  $\sigma_e$  of registration errors in millimetres and the number  $N$  of finally established *reciprocal* correspondences for different algorithms applied to different range images.

Image	Algo.	$\mu_e(mm)$	$\sigma_e(mm)$	$N$
tubby	CICP	0.26	0.16	3075
	GICP	0.29	0.17	3135
	Pulli	0.28	0.16	3147
cow	CICP	0.51	0.28	3119
	GICP	0.52	0.28	3119
	Pulli	0.52	0.29	3120
bunny	CICP	0.22	0.10	5027
	GICP	0.22	0.10	5067
	Pulli	0.22	0.10	5067